

# How to test QE neutrino-nucleus interaction model using the data QE lepton-nuclear interaction<sup>1</sup>

A.V. Butkevich

Institute for Nuclear Research of Russian Academy of Science

---

<sup>1</sup>“Sub-dominant oscillation effects in atmospheric neutrino experiments”, ICRP, 10<sup>th</sup>  
December 2004

In GeV energy region the CC QE neutrino interaction with nuclei gives main contribution to detected muons.

- Precise description of neutrino-nucleus interaction is important in analysis data used to determine neutrino properties
- The inclusive QE process  $^{16}\text{O}(\nu, \mu)$  is the main source of the '1 RING' events in water Cherenkov detector
- The semi-inclusive  $A(\nu, \mu p)B$  reactions may be observed in fine grained detector. The kinematics of an outgoing proton and lepton can be used to accurately reconstruct the energy of incoming neutrino.
- The  $A(\nu, \mu p)B$  process can be used for evaluation of non-QE interactions contribution in the '1 RING' events

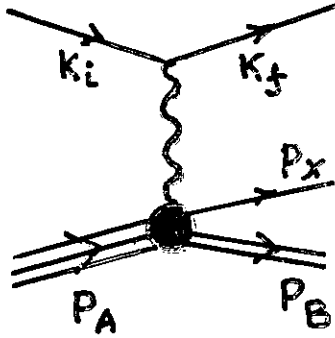
Monte-Carlo codes to simulate the response of neutrino detector are based on Fermi gas model.

- They take into account Fermi motion of the nucleons inside the nucleus and Pauli blocking effect
- The uncertainties of the existing data of QE neutrino-nucleus interaction don't allow estimate the accuracy of this model

Electron-nucleus scattering high-precision data and relativistic models.

- Fermi gas model neglect some important nuclear effects
- Relativistic Distorted Wave Impulse Approximation (RDWIA), Relativistic Optical Model Eikonal Approximation, and Relativistic Multiple Scattering Glauber Approximation (RMSGGA) explain well experimental electron QE cross-section in range of nuclei from carbon to lead

## Semi-inclusive Cross-Section



$$k_i = (\varepsilon_i, \bar{k}_i)$$

$$k_f = (\varepsilon_f, \bar{k}_f)$$

$$p_x = (\varepsilon_x, \bar{p}_x)$$

$$p_B = (\varepsilon_B, \bar{p}_B)$$

$$p_A = (m_A, 0)$$

$$q = k_i - k_f = (\omega, \bar{q}), \quad Q^2 = -q^2$$

### Electron QE scattering

$$\frac{d^6\sigma}{d\varepsilon_f d\Omega_f d\varepsilon_x d\Omega_x} = \frac{p_x \varepsilon_x \varepsilon_f \alpha^2}{(2\pi)^3 \varepsilon_i Q^4} L_{\mu\nu}^{el} (W^{\mu\nu})^{el}$$

### Neutrino QE scattering

$$\frac{d^6\sigma}{d\varepsilon_f d\Omega_f d\varepsilon_x d\Omega_x} = \cos^2(\theta_C) G^2 \frac{p_x \varepsilon_x}{(2\pi)^5} \frac{|\bar{k}_f|}{\varepsilon_i} L_{\mu\nu}^{cc} (W^{\mu\nu})^{cc}$$

$G$  is Fermi constant and  $\theta_C$  is Cabibbo angle

### Hadron tensor

$$W^{el(cc)} = \frac{1}{8m_A \varepsilon_x \varepsilon_B} \overline{\sum} \sum \int d^3\bar{p}_B |\langle B_f \bar{p}_x | J_\mu^{el(cc)} | A_i \rangle|^2 \delta(p_x + p_B - q - p_A)$$

## Lepton tensor

$$L_{\mu\nu}^{el} = l_s^{\mu\nu} + h l_A^{\mu\nu} \quad L_{\mu\nu}^{cc} = l_s^{\mu\nu} - l_A^{\mu\nu}$$

$h$  is helicity of high energy electron and  $l_S(l_A)$  is symmetrical (antisymmetrical) component

## Five-folded cross-section

For exclusive reactions in which only a single discrete state or narrow resonance of target is excited ( $^{16}\text{O}(e, e'p)^{15}\text{N}$  or  $^{16}\text{O}(\nu, \mu p)^{15}\text{O}$ ) we use recoil factor

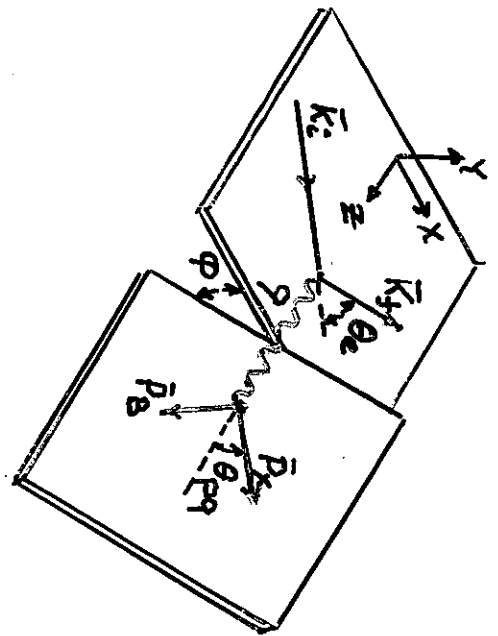
$$R = \int \delta(\varepsilon_x + \varepsilon_B - \omega - m_A) d\varepsilon_x = \left| 1 - \frac{\varepsilon_x (\bar{p}_x \bar{p}_B)}{\varepsilon_B p_x^2} \right|^{-1}$$

and obtain cross-section in form

$$\frac{d^5 \sigma^{el}}{d\varepsilon_f d\Omega_f d\Omega_x} = R \frac{p_x \varepsilon_x}{(2\pi)^3} \frac{\varepsilon_f}{\varepsilon_i} \frac{\alpha^2}{Q^4} L_{\mu\nu}^{el} (W^{\mu\nu})^{el}$$

$$\frac{d^5 \sigma^{cc}}{d\varepsilon_f d\Omega_f d\Omega_x} = R \cos^2(\theta_C) G^2 \frac{p_x \varepsilon_x}{(2\pi)^5} \frac{k_f}{\varepsilon_i} L_{\mu\nu}^{cc} (W^{\mu\nu})^{cc}$$

In electron scattering experiments the five-fold cross-section is measured holding variables  $(\omega, q)$  and  $p_x$  fixed.



## Inclusive cross-section

In reference frame

$$\hat{z} = \bar{q}/|\bar{q}| \quad \hat{y} = \bar{k}_i \times \bar{k}_f / |\bar{k}_i \times \bar{k}_f|$$

the inclusive cross-sections have form

$$\frac{d^2\sigma^{el}}{d\varepsilon_f d\Omega_f} = \sigma_M \{V_L R_L + V_T R_T\}$$

where the Mott cross-section

$$\sigma_M = \alpha^2 \cos^2(\theta/2) / 4\varepsilon_i^2 \sin^4(\theta/2)$$

$$\frac{d^2\sigma^{cc}}{d\varepsilon_f d\Omega_f} = \cos^2(\theta_C) \frac{G^2}{4\pi^2} |\bar{k}_f| \varepsilon_f \{V_L R_L + V_T R_T + V_{zz} R_{zz} - V_{0z} R_{0z} \pm V_{xy} R_{xy}\}$$

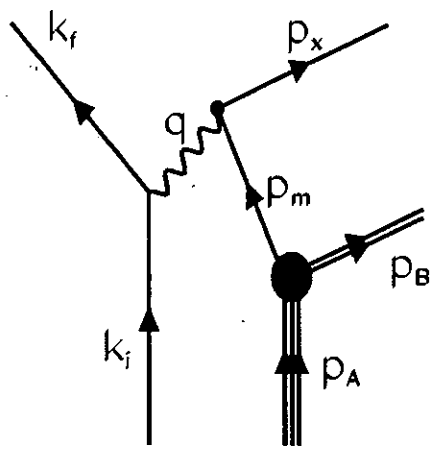
Nuclear response functions

$$\begin{aligned} R_L &= W^{00} \sim \langle J^0(J^0)^+ \rangle \\ R_T &= W^{xx} + W^{yy} \sim \langle J^x(J^x)^+ \rangle + \langle J^y(J^y)^+ \rangle \\ R_{0z} &= W^{0z} + W^{z0} \sim \langle J^0(J^z)^+ \rangle + \langle J^z(J^0)^+ \rangle \\ R_{xy} &= i(W^{yx} - W^{xy}) \sim 2\text{Im}(\langle J^y(J^x)^+ \rangle) \end{aligned}$$

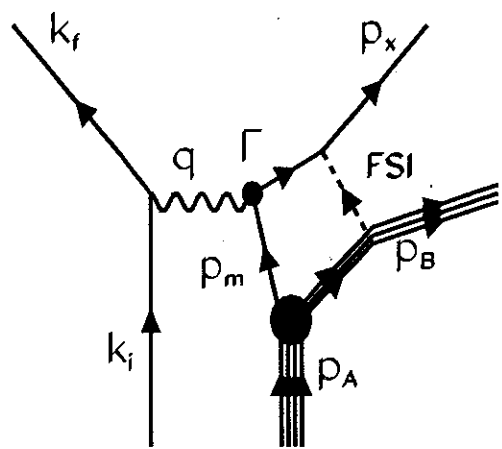
The coefficients obtained from lepton tensor

$$\begin{aligned} V_L &= 1 + \tilde{k} \cos(\theta) \\ V_T &= 1 - \tilde{k} \cos(\theta) + \frac{\varepsilon_i |\bar{k}_f| \tilde{k}}{|\bar{q}|^2} \sin^2(\theta) \end{aligned}$$

RPWIA



RDWIA





# RDWIA

Bound nucleon wave functions

$$\Psi_i(r) = \begin{pmatrix} u_i \\ v_i \end{pmatrix}$$

are the solution of a Dirac equation, derived within relativistic mean field approach from a relativistic Lagrangian with scalar and vector potentials.

Ejectile nucleon wave functions

$$\Psi_f(r) = \begin{pmatrix} \psi_+ \\ \psi_- \end{pmatrix}$$

can be written as

$$\Psi_f(r) = \begin{pmatrix} \psi_+ \\ \frac{\vec{\sigma} \cdot \vec{p}}{E+M+S-V} \psi_+ \end{pmatrix}$$

where  $S$  and  $V$  are scalar and vector components of phenomenological optical potential of nuclei with energy  $E$ . The range applicability  $A=12 \div 208$  and energies  $E=20 \div 1040$  MeV.

$\psi_+$  can be related with a two-component wave function  $\Phi$  by Darwin factor  $D(r)$

$$\Psi_+ = D^{1/2} \Phi$$

$$D(r) = [E + M + S(r) - V(r)] / (E + M)$$

and  $\Phi$  is solution of Schrodinger equation.

## Vertex operators for nucleon current

The electromagnetic vertex function  $\Gamma^\mu$  for a free nucleon can be represent by three different operator which a related by Gordon identity. Usually cc2 definition is used

$$\Gamma_\mu^{el} = F_1(Q^2)\gamma_\mu + i\frac{k}{2M}F_2(Q^2)\sigma_{\mu\nu}q^\nu$$

where  $F_1$  and  $F_2$  are Dirac and Pauli nucleon form-factors,  $k$  is anomalous magnetic moment, and  $\sigma_{\mu\nu} = \frac{i}{2}[\gamma_\mu\gamma_\nu]$ .

Current conservation is restricted by replacing

$$J^z = \frac{\omega}{|\vec{q}|} J^0$$

The charge current vertex function

$$\Gamma_\mu^{cc} = F_1^V(Q^2)\gamma_\mu + \frac{i}{2}F_2^V(Q^2)\sigma_{\mu\nu}q^\nu - G_A(Q^2)\gamma_\mu\gamma_5 + F_p(Q^2)q_\mu\gamma_5$$

where  $F_1^V$  and  $F_2^V$  are isovector Dirac and Pauli nucleon form-factors,  $G_A$  and  $F_p$  are axial and psevdoscalar form-factors and

$$G_A = \frac{g_A}{(1 + Q^2/M_A^2)^2} \quad F_p = \frac{2MG_A}{m_\pi^2 + Q^2}$$

$m_\pi$  and  $M_A$  are the pion and axial masses respectively,

$$g_A = 1.267$$

$$V_{zz} = \mathbb{I} + \tilde{k} \cos(\theta) - 2 \frac{\varepsilon_i |\bar{k}_f| \tilde{k}}{|\bar{q}|^2} \sin^2(\theta)$$

$$V_{0z} = \frac{\omega}{|\bar{q}|} (\mathbb{I} + \tilde{k} \cos(\theta)) + \frac{m_l^2}{|\bar{q}| \varepsilon_f}$$

$$V_{xy} = \frac{\varepsilon_i + \varepsilon_f}{|\bar{q}|} (\mathbb{I} - \tilde{k} \cos(\theta)) - \frac{m_l^2}{|\bar{q}| \varepsilon_f}$$

where  $\tilde{k} = |\bar{k}| / \varepsilon_i$

## Current operator in Impulse Approximation

The current matrix element  $J^\mu$  calculate in framework of the Impulse Approximation. In this model it is assumed

- incident lepton interacts with only one nucleon
- nuclear current is the sum of single nucleon currents

$$J^\mu(\bar{q}) = \sum_{i=1}^A j_i^\mu(\bar{q})$$

- the states of the target and residual nuclei describe by independ particle model wave functions

Matrix elements of the nuclear current operator in relativistic model

$$J^\mu(\bar{q}) = \int d\bar{r} \bar{\Psi}_f(\bar{r}) \Gamma^\mu(\bar{q}) \exp(i\bar{q}\bar{r}) \Psi_i(\bar{r})$$

is calculated with relativistic wave functions for initial bound  $\Psi_i$  and final scattering  $\bar{\Psi}_f$  states

## PWIA

In Plane Wave Impulse Approximation (PWIA) the knockout  $A(e, e' p)B$  cross-section factorizes in form

$$\frac{d\sigma}{d\varepsilon_f d\Omega_f d\varepsilon_x d\Omega_x} = \frac{\varepsilon_x p_x}{(2\pi)^3} \sigma_{eN} S(E_m, P_m)$$

where  $\sigma_{eN}$  is the cross-section for scattering of an electron by the off-shell nucleon.

$S(p_m, E_m)$  is probability that removal of a nucleon with momentum  $p_m$  will result in final state of residual nuclei with missing energy  $E_m = M_B + M - M_A$

In PWIA the momentum distribution  $\rho(p_m)$  for a fully occupied orbital with total angular momentum  $j$  is normalized to its occupancy

$$4\pi \int dp_m \rho_j(p_m) p_m^2 = 2j + 1$$

From measured cross-section the distorted momentum distribution

$$\rho^D(\bar{p}_m, \bar{p}_x) = \frac{(2\pi)^3}{\varepsilon_x p_x} \frac{1}{\sigma_{eN}} \frac{d\sigma}{d\varepsilon_f d\Omega_f d\varepsilon_x d\Omega_x}$$

can be obtained.

The main states and measured occupancy of  $^{16}\text{O}$   
Ip1/2 discrete state -  $E_m = 12.13$  MeV and  $n_\alpha \approx 1.4$   
Ip3/2 discrete state -  $E_m = 18.45$  MeV and  $n_\alpha \approx 2.6$   
Is1/2 continue state -  $E_m \approx 40.2$  MeV and  $n_\alpha \approx 2$

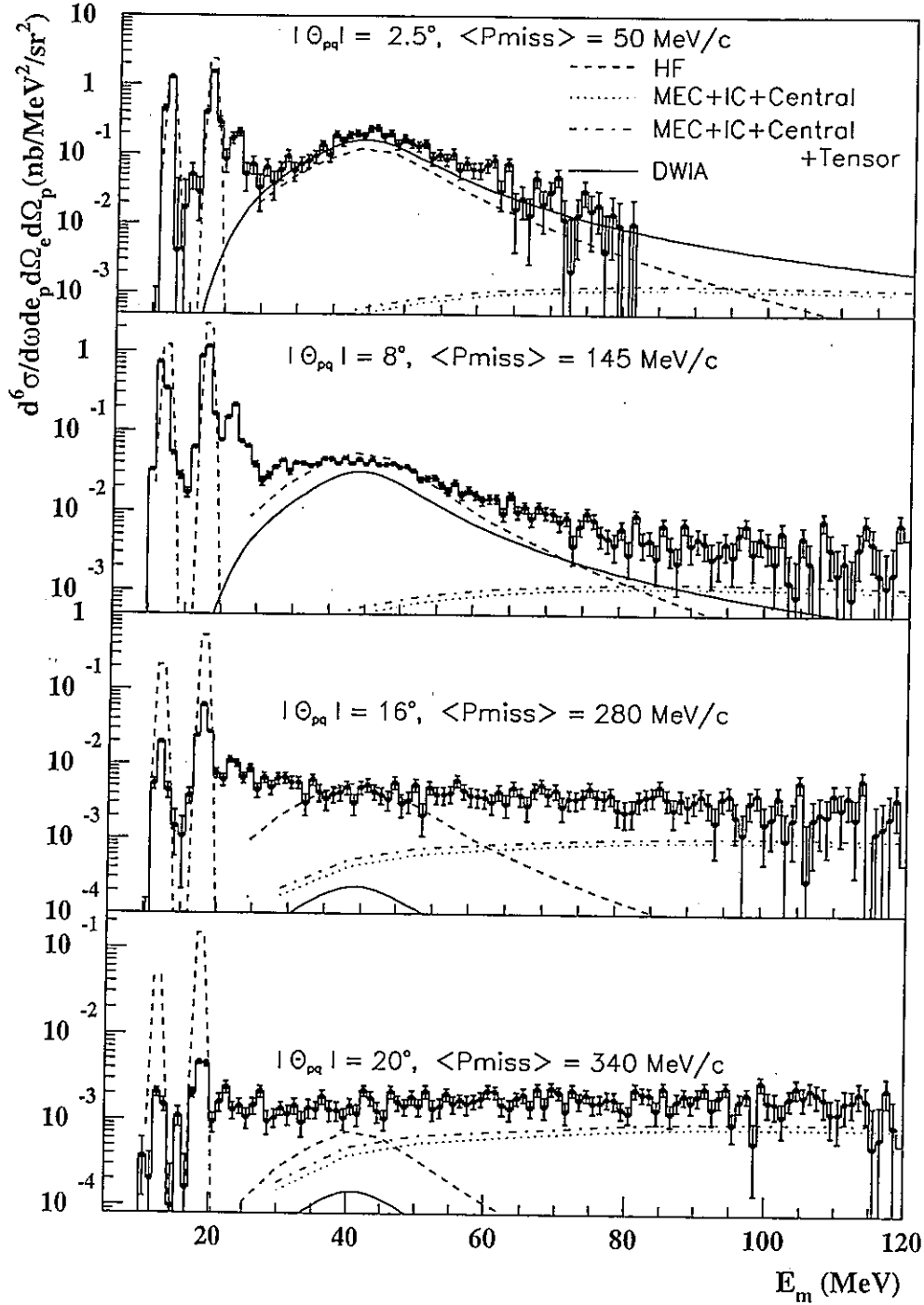


Fig. 5. Six-fold differential  $^{16}\text{O}(e, e'p)$  cross sections as a function of missing energy for four different average values of missing momentum. The solid (dashed) lines represent the Kelly [9] (Ryckebusch *et al.* [16,24-27]) single nucleon knockout calculations folded with the Lorentzian parameterization of Mahaux [28]. The dotted Ryckebusch *et al.* calculation shows the  $(e, e'pp)$  and  $(e, e'pn)$  contributions due to pion-exchange currents, intermediate  $\Delta(1232)$  creation, and central short-range correlations, while the dot-dashed calculation also includes tensor correlations. The prominence of the broad peak centered at  $E_{\text{miss}} \approx 40$  MeV, which is primarily due to knockout from the  $1s_{1/2}$ -state, decreases with increasing  $p_{\text{miss}}$ . Figure courtesy N. Liyanage.

## RESULT

Several codes have been developed based on RDWIA model and applied to QE electron scattering data.

- Jefferson Lab. Experiment E89-003  $^{16}\text{O}(e, e'p)^{15}\text{N}$ ,  
 $E_e=2.442\text{GeV}$ ,  $\theta_e=23.36^\circ$ ,  $Q^2=0.8\text{GeV}^2$   
(K.G.Fissum et al. nucl-ex/0401021)

Calculations are given by J.Kelly (Phys.Rev.C60,044609, (1999)) and J.M.Udias et al. (Phys.Rev.Lett. 83,5451, (1999)).

Normalization factors are 0.73 and 0.72 for  $1p_{1/2}$  and  $1p_{3/2}$  states

- Kelly's result in comparison with different data sets
- Inclusive cross-sections calculated by A.Meucci et al. (Phys.Rev. C67,054601,2003) in comparison with  $^{16}\text{O}(e, e')$  data of ADONE-Frascati experiment (M.Anghinolfi et al. (Nucl.Phys. A602,405 (1996)) and predictions of RFGM ( $P_F=225\text{ MeV}$ ,  $\epsilon_B=27\text{ MeV}$ )
- Meucci et al. (Nucl.Phys. A739,277,2044)  
The flux-averaged (Los-Alamos neutrino spectrum) QE cross-section integrated over the muon energy gives  $11.15 \times 10^{-40}\text{ cm}^2$  and experimental value of  $(10.6 \pm 0.3 \pm 1.8) \times 10^{-40}\text{ cm}^2$  (L.B.Auerbach et al. Phys.Rev. C66,015501 (2002)) ;  $^{12}\text{C}(\nu_\mu, \mu)$

- Meucci et al.  $R = \sigma_{DWIA}/\sigma_{PWIA} \approx 0.66$  at  $E_\nu = 0.3$  GeV and  $R \approx 0.81$  at  $E_\nu = 1$  GeV  
Maieron et al.  $R = \sigma_{DWIA}/\sigma_{RFGM} \approx 1$  at  $E_\nu = 0.3$  GeV and  $R \approx 0.85$  at  $E_\nu = 1$  GeV (nucl-th/0407094)
- $\sigma_{Meucci}/\sigma_{Maieron} \approx 0.7$  at  $E_\nu \geq 0.3$  GeV

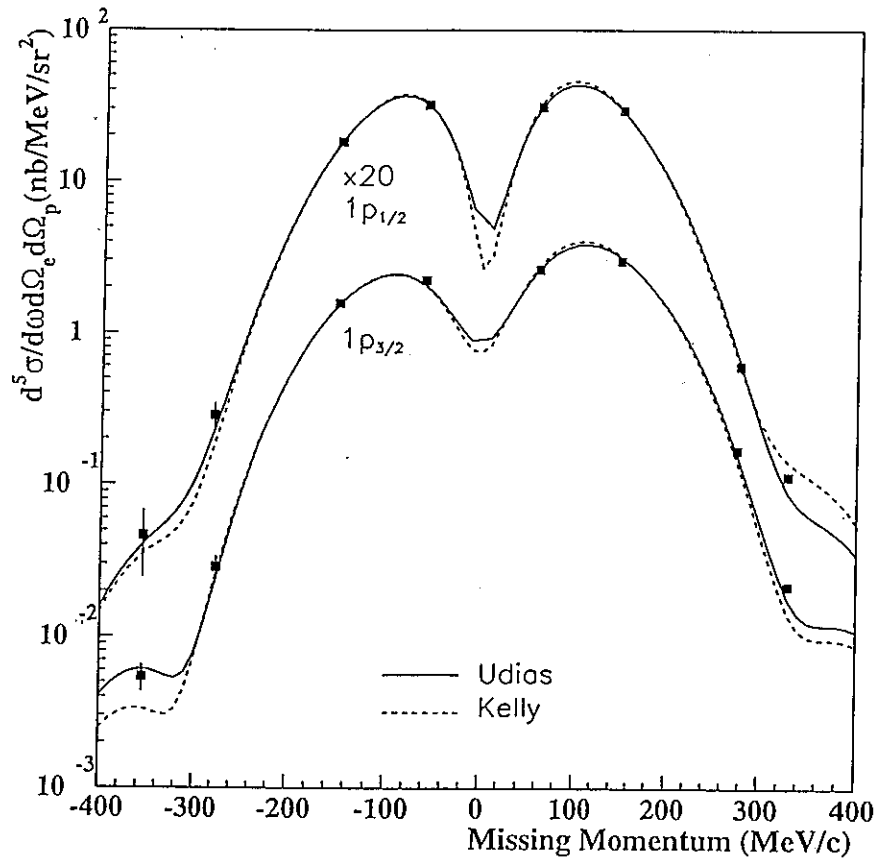
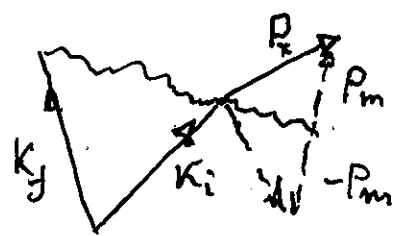


Fig. 2. Five-fold differential cross sections obtained in perpendicular kinematics for the knockout of  $1p$ -shell protons from  $^{16}\text{O}$  as a function of missing momentum. Details pertaining to the calculation represented by the solid (dashed) line may be found in [20] ([9]). Figure courtesy J. Gao.





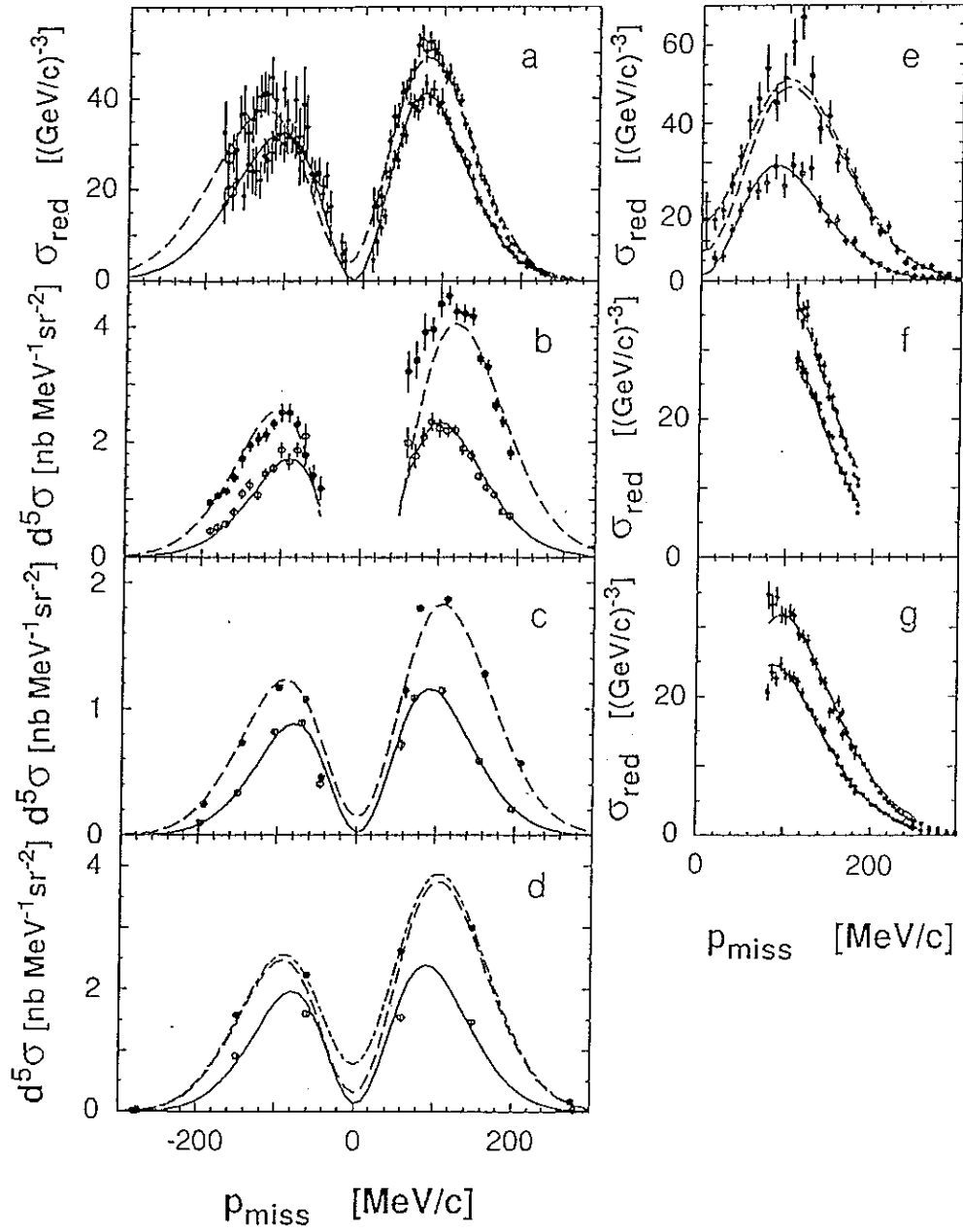
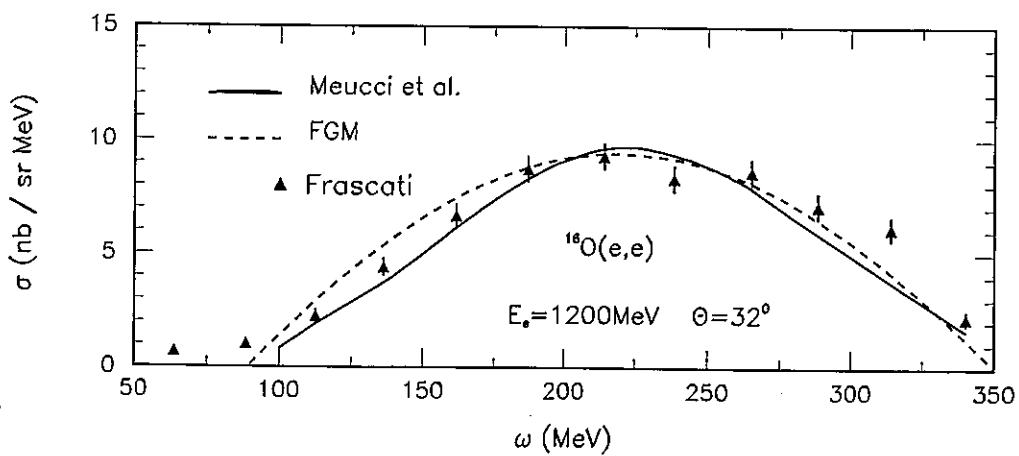
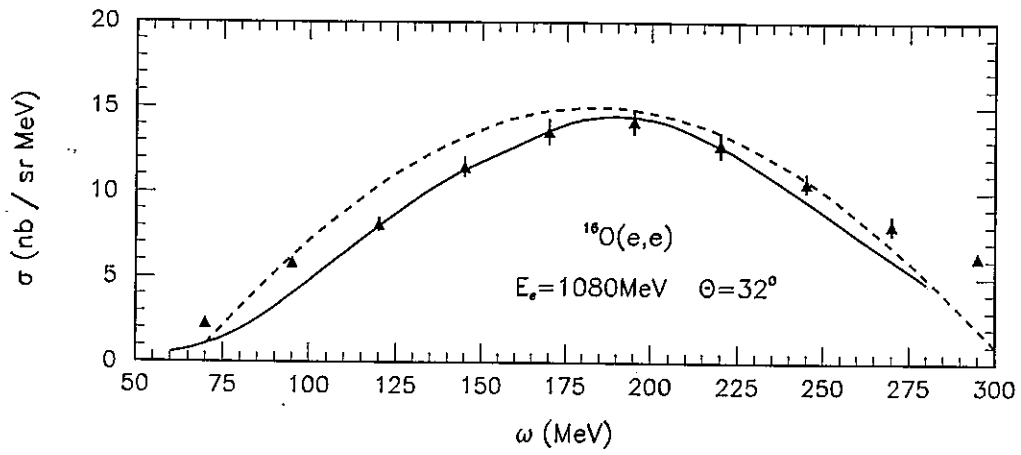
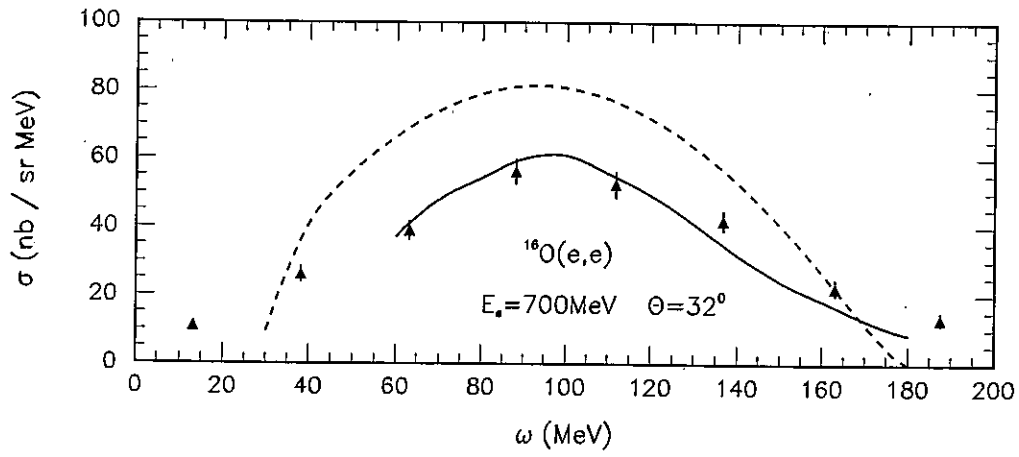
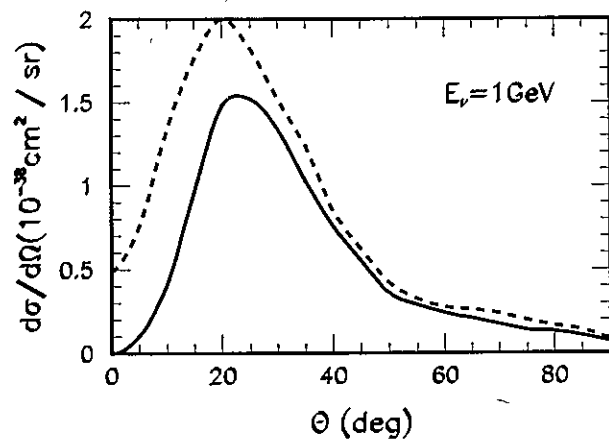
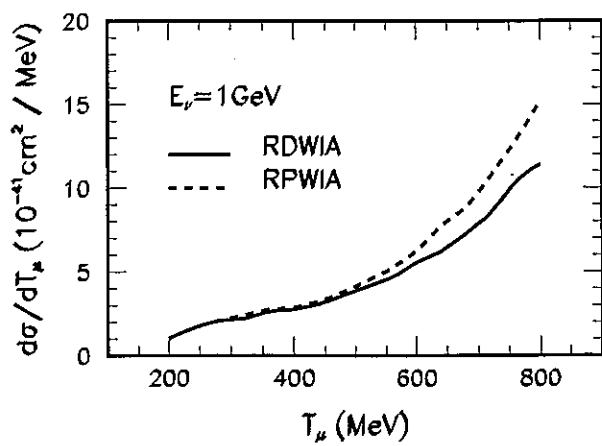
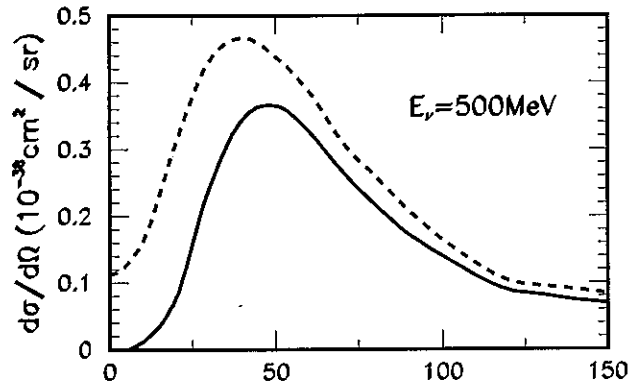
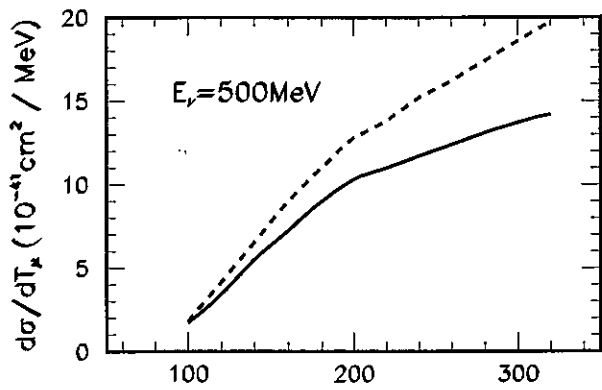
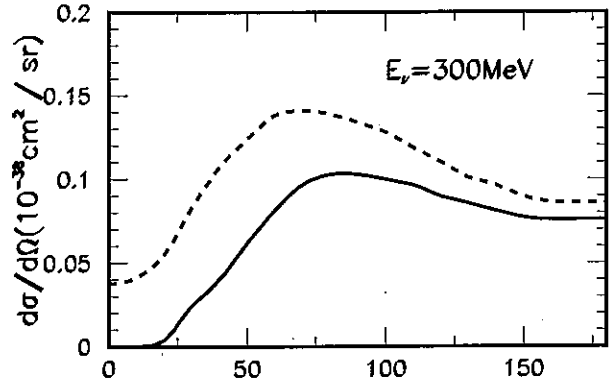
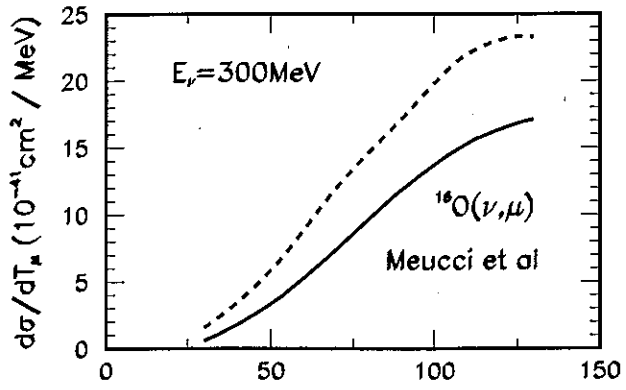
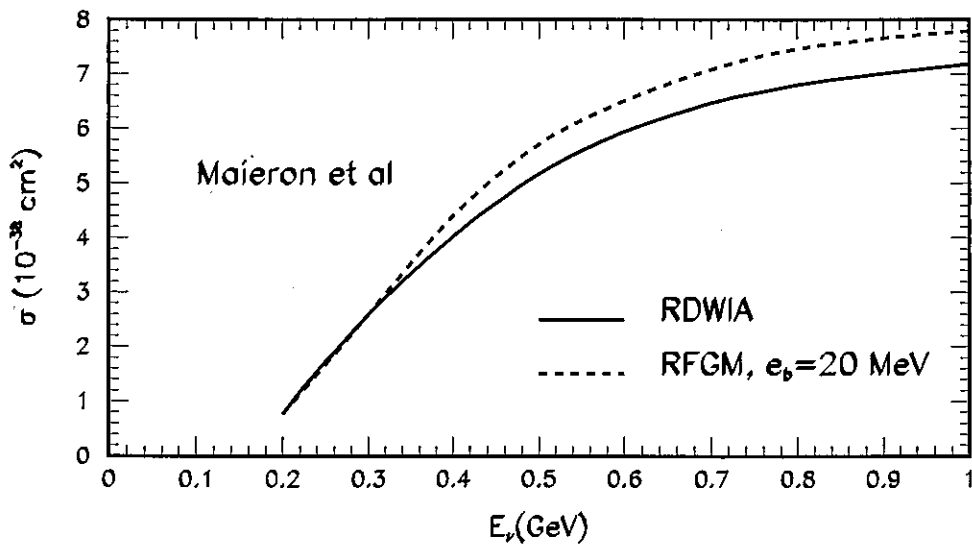
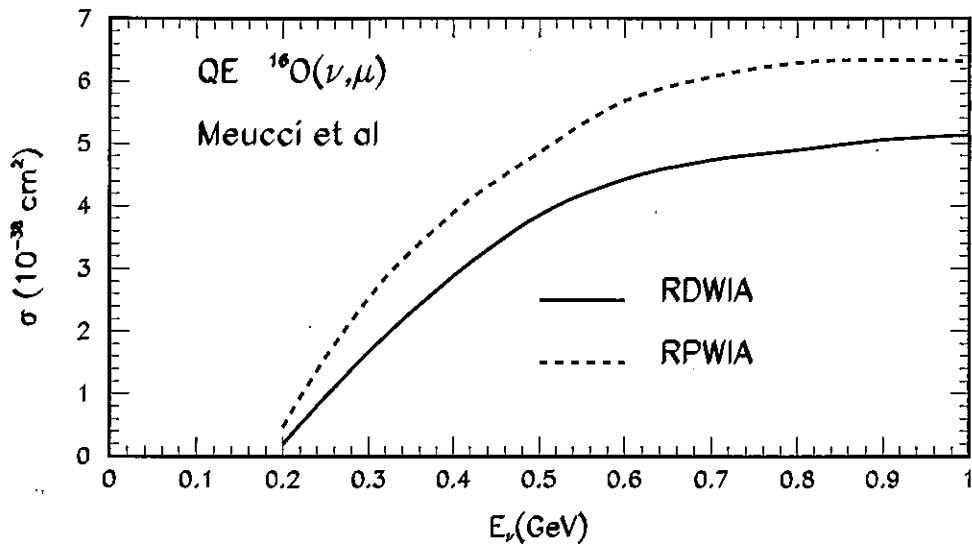


FIG. 24: Fits to various  $^{19}\text{O}(e, e'p)$  data sets based on the HS bound-nucleon wave function and the EDAD1 optical potential. See Table IX for the key to the data-set labels. Open points and solid lines pertain to the  $1p_{1/2}$ -state, while solid points and dashed lines pertain to the  $1p_{3/2}$ -state. The dashed-dotted lines include the contributions of the positive parity  $2s_{1/2}/d_{3/2}$ -doublet to the  $1p_{3/2}$ -state. Panel (d) shows the data from this work.







## Conclusion

- RDWIA model explains well the the experimental electron-nuclei QE cross-sections.
- Comparison of RDWIA, RPWIA, and RFGM predictions with  $^{16}\text{O}$  data shows that FSI effects are significant at electron energies less then 1 GeV.
- Two calculations of QE neutrino-nuclei cross-sections in the framework of RDWIA model predict different (%30) results. But RPWIA and RFGM results are always large.
- New careful calculations are required.